Large-pitch steerable synthetic transmit aperture imaging (LPSSTA)

Ying Li, Michael C. Kolios, and Yuan Xu*

Department of Physics, Ryerson University
Institute for Biomedical Engineering, Science and Technology (iBEST), a partnership between Ryerson University and St. Michael's Hospital
Keenan Research Centre for Biomedical Science of St. Michael's Hospital
*yxu@ryerson.ca

ABSTRACT

A linear ultrasound array system usually has a larger pitch and is less costly than a phased array system, but loses the ability to fully steer the ultrasound beam. In this paper, we propose a system whose hardware is similar to a large-pitch linear array system, but whose ability to steer the beam is similar to a phased array system. The motivation is to reduce the total number of measurement channels M (the product of the number of transmissions, n_T, and the number of the receive channels in each transmission, n_R), while maintaining reasonable image quality. We combined adjacent elements (with proper delays introduced) into groups that would be used in both the transmit and receive processes of synthetic transmit aperture imaging. After the M channels of RF data were acquired, a pseudo-inversion was applied to estimate the equivalent signal in traditional STA to reconstruct a STA image. Even with the similar M, different choices of n_T and n_R will produce different image quality. The images produced with $M=N^2/15$ in the selected regions of interest (ROI) were demonstrated to be comparable with a full phased array, where N is the number of the array elements. The disadvantage of the proposed system is that its field of view in one delay-configuration is smaller than a standard full phased array. However, by adjusting the delay for each element within each group, the beam can be steered to cover the same field of view as the standard fully-filled phased array. The LPSSTA system might be useful for 3D ultrasound imaging.

Keywords: spatially encoding, pseudoinverse, sparse array, elements combination, beam steering

1. INTRODUCTION

To generate a 3D ultrasound image, a 2D transducer array is usually required. To avoid the grating lobe artifacts, the inter-element pitch of the array has to be less than half a wavelength.[1] Even though a linear array system costs less compared to a full phased array system, the steering and focusing of the linear array is usually limited to the direct forward direction of the array.[2] When the number of active channels is large, the cost of the hardware system will be prohibitively high due to the electronics associated with each element.[3] Therefore, many innovations in designing an effective sparse array have been investigated.[4-12] However, the quality of images cannot be preserved due to the reduction of the number of elements. There are grating lobes when using a periodic sparse array, while random sparse arrays suffer from the significant side lobes.[13]

Liu has proposed an idea to change the element spacing on both transmit and receive by tying the elements into groups to reduce the negative effects of grating lobes.[5] Lockwood *et al*.[6] proposed a framework of designing sparse linear arrays. For conventional B-mode ultrasound imaging system, they suggested that arranging the element spacing properly can optimize the two-way radiation pattern to avoid the grating lobes. They also applied similar methods to achieve a desired effective aperture by transmitting from five virtual elements and receiving signals with a properly apodized full aperture in 3-D STA imaging.[1] In addition, the coherent array imaging method with the subarray techniques[14] has been proposed to reduce the number of coaxial cables in the probe cable while maintaining the image quality of a full phased array imaging system.

In this paper, we propose a new approach, which is similar to a large-pitch linear array system but can steer the ultrasound beam like a phased array system. When the adjacent elements of a phased array are combined as a group in both transmit and receive, the inter-group pitch (the distance between the adjacent groups) will be larger than half a

Medical Imaging 2016: Ultrasonic Imaging and Tomography, edited by Neb Duric, Brecht Heyde, Proc. of SPIE
Vol. 9790, 97901Y · © 2016 SPIE · CCC code: 1605-7422/16/$18 · doi: 10.1117/12.2216908

wavelength, which normally introduces grating lobes. However, the beam pattern or the directivity of a group will cancel the grating lobes, thus maintaining an acceptable image quality. For the normal large-pitch linear array system, the beam cannot be steered by the simple combination and the ROI is limited to the region right under the probe. To solve this problem, we will add appropriate delays among the elements of each group to steer the beam.

In Section 2, the encoding process of the proposed method will be presented. In Section 3, the implementation of the encoding will be described and simulation parameters stated. Image quality metrics will be shown and applied to the reconstructed images. In Section 4, the image quality of the simulated images from our proposed method will be assessed and compared to the standard STA. The discussion and conclusion will be presented in Section 5.

2. METHODS

2.1 Encoding operator

Assume the probe array has N elements, and there are L transmissions to acquire one frame. We can define an L-by-N matrix $\mathbf{T}$ to describe the transmission encoding in a format similar to the delay-encoded synthetic transmit aperture imaging (DESTA) [15]. K receiving groups/channels are used in each transmission. Define $\mathbf{R}$ as an N by K matrix to encode the receiving elements in a similar way. In each transmission, one group will transmit a wave, and all groups will receive the signals. The encoding protocol changes a full phased array system into a large-pitch array system. The encoding process in both transmit and receive can be described as

$$\mathbf{TS}(t)\mathbf{R} = \mathbf{M}(t), \tag{1}$$

where $\mathbf{S}(t)$ is the equivalent traditional STA signal matrix from a full phased array system, with a size N by N, and $S_{ij}(t)$ is the signal at t received by the j-th element when the i-th element transmits. $\mathbf{M}(t)$ is a measurement matrix or the traditional STA signal matrix from the large-pitch array system, and $M_{ij}(t)$ is the signal at t received by the j-th group when the i-th group transmits. $\mathbf{T}$ and $\mathbf{R}$ can be defined in the frequency domain if a delay is used in the encoding.[15]

The transmission and receiving encoding process could be represented in a Kronecker product using a mathematical identity.[16] Therefore, an encoding operator can be defined as

$$\mathbf{E} = \mathbf{R}^T \otimes \mathbf{T}, \tag{2}$$

where the superscript T means the transpose of the matrix. Thus, this encoding operator can be applied to the traditional STA signal. Note that to apply this operator properly, the traditional STA signals $\mathbf{S}(t)$ and $\mathbf{M}(t)$ have to be vectorized into column vectors $\mathbf{S}_{vector}(t)$ and $\mathbf{M}_{vector}(t)$ by stacking the columns of the corresponding matrix, respectively. We have

$$\mathbf{E}\mathbf{S}_{vector}(t) = \mathbf{M}_{vector}(t) \tag{3}$$

Equation (3) will form a linear equation set for all the L transmission events. To recover $\mathbf{S}$ from $\mathbf{M}$, pseudo-inversion with regularization can be used. When a delay was applied to the encoding, the above equation can be transformed into the frequency domain and each frequency component can be decoded separately.[15]

2.2 Encoding schemes

To encode the receiving signals, k adjacent elements are combined together as one receiver (k can be an arbitrary integer) by summing the signals from the k elements after applying proper delay to each element to steer the beam to a desired angle. For example, k=5 represents five elements combined as one group to produce one signal channel. The first group includes the elements from the 1st one to the 5th one. This will reduce the receiving channels from N to about N/k. Note that, in this paper, if N/k is not an integer, there are (k+mod (N,k)) (mod is the modulo function) elements in the last group of elements. We will first use the case without steering the beam to illustrate the construction of $\mathbf{T}$ and $\mathbf{R}$. To image a ROI directly under the array, the receiving encoding matrix $\mathbf{R}$ is defined as

$$\mathbf{R} = \mathbf{I}_{N/k} \otimes \mathrm{V}_k, \tag{4}$$

where $\mathbf{I}$ is the identity matrix with the size of N/k, V_k is a k-order column vector of all ones, and $\otimes$ represents the Kronecker product.

Similarly, in the transmission mode, l adjacent elements in one group can also be combined to be excited by one source with applying proper delay to each element of the group to steer the beam to a desired angle. If N/l is not an integer, (l+mod(N,l)) elements will be combined together in the last group. This transmission-encoding matrix **T** can be written as,

$$\mathbf{T} = \mathbf{I}_{N/l} \otimes \mathrm{V}_l^T , \tag{5}$$

where **I** is the identity matrix with the size of N/l. Therefore, the number of transmissions can be reduced to N/l. In this paper k and l were chosen to be relatively prime to each other to achieve the optimized grating-lobe reduction.

The disadvantage of the proposed approach is that its field of view in one delay-configuration is smaller than a standard fully sampled phased array. However, the delay applied to the element at x, $D(x)$, can be adjusted to steer the probe array to a certain angle θ_s. In this paper, the choices of steered angles were determined by the pitch of the groups, p, as follows to reduce the grating lobes

$$\theta_s = \sin^{-1}(\frac{n\lambda}{p}) \ (n = 0, 1, 2, \ldots) , \tag{6}$$

where n is an integer and λ is the wavelength corresponding to the central frequency of the array. The delay will be applied in both the transmission and the reception process. Generally, the steering angle of the transmit and receive can be slightly different to achieve the optimized grating lobe suppression in the case that the group pitches in transmit and receive are different. The center of each group was used as the reference point with the delay to be zero. Therefore, the delay can be calculated as

$$D(x) = \delta_x \sin\theta_s / c , \tag{7}$$

where δ_x is the distance between the center of the element at x to the center of the group, and c is the speed of sound. Equation (6) and (7) can be combined to obtain the $D(x)$ as

$$D(x) = \frac{n\delta_x\lambda}{pc} \quad (n = 0, 1, 2, \ldots.). \tag{8}$$

Note that, $D(x)$ can be used to construct the encoding operator **E**, which is similar to the delay matrix in DESTA.[15]

2.3 The number of measurement channels

Based on the transmission and receiving encoding schemes, the total number of measurement channels can be calculated by the product of the number of receiving channels and the number of transmission events:

$$M = n_T n_R , \tag{9}$$

where $M < N^2$. In this paper, several combinations in transmit elements and receive elements were tested. For each scenario, M was similar, but n_T and n_R varied. Note that we used M because when the number of transmissions is increased, the active receiving channel can be reduced to have a similar M. In the decoding process, a pseudo-inversion was used to estimate the equivalent signal in traditional STA from the acquired measurement data. In this paper, we used the conjugate transpose of the encoding operator **E** to approximate the pseudo-inversion to simplify the decoding process.

3. SIMULATION METHODS

3.1 Simulation parameters

The FIELD II program was used to generate the standard STA RF data.[17] The probe was a 128-element, 2-cm wide, 5-MHz phased array with a 0.15-mm pitch, 0.01-mm kerf and 10-mm height. The sampling frequency was 40 MHz.

3.2 Simulation phantoms

There were two simulated phantoms in our simulations. The first one is 2 cm ×1 cm × 2 cm (Azimuth × Elevational × Axial), and contains five point targets placed at 4 mm apart from 7 mm to 23 mm depth. The second one is 6 cm ×1 cm × 6 cm (Azimuth × Elevational × Axial), with thirty-five 5-mm-diameter hypo-echoic inclusions placed in five rows from top to bottom, and the centers are at 1.5 cm, 2.5 cm, 3.5 cm, 4.5 cm, and 5.5 cm depth. For each row, the centers of the middle three hypo-echoic lesions are separate by 6 mm apart horizontally. The simulated probe was placed from 2 cm to 4 cm laterally, and 0.5 cm away from the top of the simulated medium. The log-enveloped beamformed images were displayed after applying the Hilbert transform and logarithm compression.

3.3 Imaging quality metrics

Clutter-energy-to-total-energy ratio (CTR) was used to evaluate the ability of an imaging system to detect anechoic objects in the presence of strongly scattering off-axis objects

$$\mathrm{CTR} = 10\log_{10}\left\{1-\frac{\int_{x,z\in R}|I(x,z,x_0,z_0)|^2}{\int|I(x,z,x_0,z_0)|^2}\right\} \tag{10}$$

where (x_0, z_0) is the center of the point scatter, the radius R of the image region was chosen as 5 wavelengths.[18]

4. RESULTS

Figure 1 exhibits the log-enveloped beamformed images with various pairs of (n_T, n_R) (the pairs are listed above each image) and the line plots (the bottom row) through the center of the middle point target with a similar number of measurement channels (M). Figure 1(a) is the standard STA image of a full phased array, shown as the reference. Figure 1 (b) and (c) are the images with (n_T, n_R) equal to (N/3, N/5) and (N/4, N/4), respectively. More artifacts can be found in the image and the line plot of (N/4, N/4) configuration than those of (N/3, N/5) configuration. The CTR of the middle point target in the image of (N/3, N/5) is -35.42 dB and comparable to that of the reference image, -39.14 dB, and is significantly better than that of (N/4, N/4) configuration, -23.80 dB.

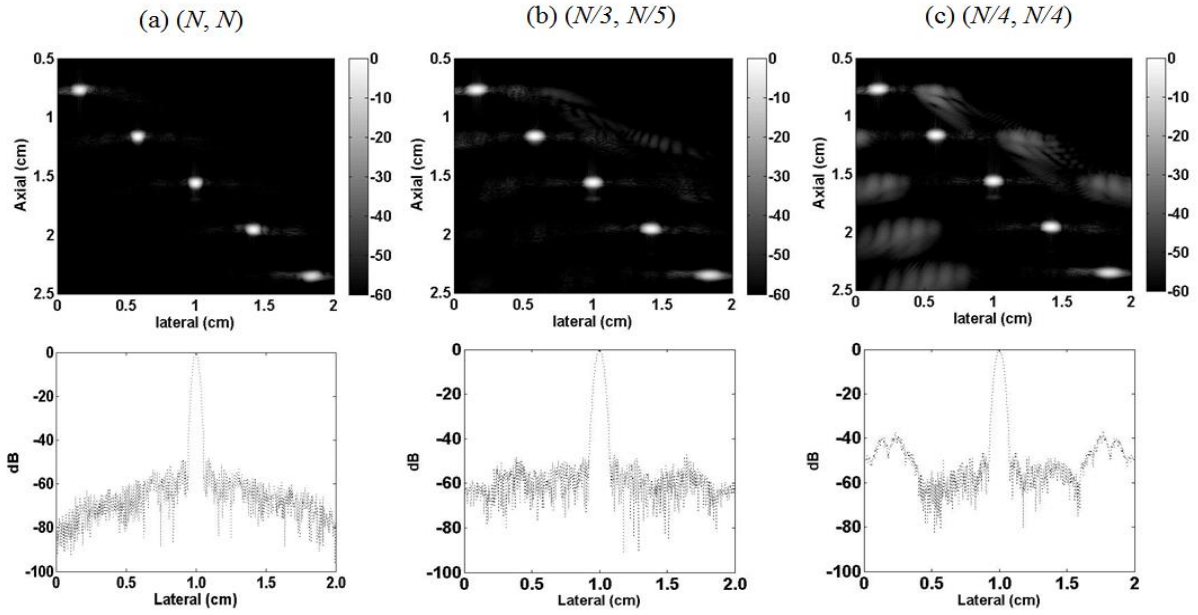

Figure 1. Log-enveloped images obtained from various (n_T, n_R) configurations: (a) (N, N), (b) (N/3, N/5) and (c) (N/4, N/4). Top row: point targets phantom images. Bottom row: lateral line plots at 1.5 cm depth (through the center of the middle point scatter).

Figure 2 shows the beamformed images obtained from various steering angles with the same element combination scheme. Four elements are combined as one group in both the transmission and the reception process. Figure 2 (a) is the beamformed image without delay added to elements ($\theta_s = 0^o$). With the element combination in both transmission and reception, the ROI was restricted to the region directly underneath of the probe. Figure 2 (b) and (c) show the results of steering the probe array to the left and to the right, with a 30-degree angle, respectively. The dynamic apodization was applied to all the three images. After adding the delay, the image quality is comparable with the case without steering.

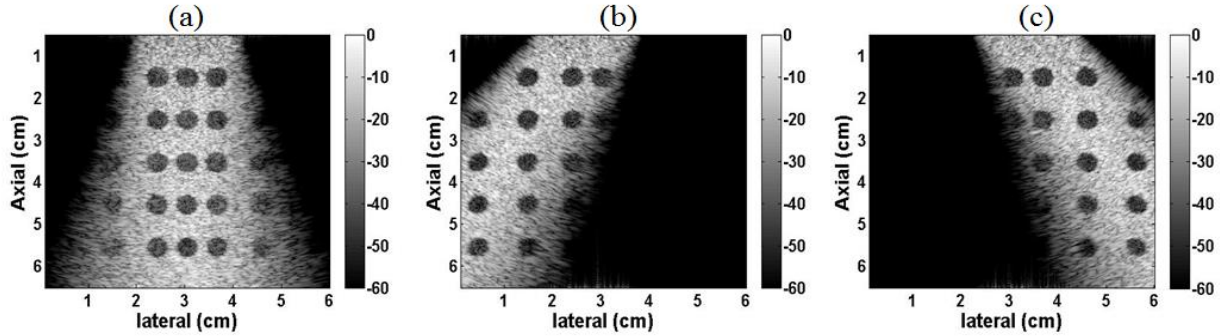

Figure 2. Images obtained with the (*N*/4, *N*/4) configuration for various steering angles of (a) $\theta_s = 0^o$ (No delay added), (b) $\theta_s = 30^o$ to the left, and (c) $\theta_s = 30^o$ to the right.

5. SUMMARY AND CONCLUSION

When multiple adjacent elements are combined together as one group, the array pitch will be increased to more than half a wavelength, which will result in the appearance of grating lobes even after the suppression due to the directivity of the group. Our results show that the (*N*/3, *N*/5) configuration yields a better image than the (*N*/4, *N*/4) configuration. This might be explained by the effective aperture theory.[6] Moreover, the reconstruction images in the specified ROI from the (*N*/3, *N*/5) configuration, in which the total number of active RF channels is only one-fifteenth of that of the full phased array, are comparable to those of the full phased array.

By adjusting the appropriate delay to each element in each group, the probe array can be steered to a certain angle to achieve the similar ROI as that in a standard phased array system. The selection of the steered angles is determined by the pitch of the group. Generally, the combinations of n_T and n_R can be selected following the design of effective aperture.[6] In the future, other possible selections of (n_T, n_R) with delays will be investigated to optimize the image quality.

Alternatively, to overcome the loss in SNR of the RF signals in STA, multiple group excitation in one transmission can be encoded using spatial encoding methods, such as DE-STA to increase the transmit power in STA.[15] Furthermore, this proposed approach can be applied in both the lateral and the elevational direction of the 2D array of a 3D ultrasound imaging. This might not only achieve a high image quality for a specific field of view, but also significantly decrease the cost of a 3D ultrasound imaging system.

In conclusion, a large-pitch array system with steerable field of view is presented. Even with a similar number of measurement channels, different element combination schemes in the transmission and the reception process produced different image qualities. By reducing the number of measurement channels and the transmission events, the cost and the complexity of the imaging system can decrease due to the fewer electronics associated with each element. Although the initial simulations were implemented in 2D STA, this method can be extended to 3D STA imaging system.

6. ACKNOWLEDGMENT

The authors would like to thank the following funding agencies: Natural Sciences and Engineering Research Council of Canada (NSERC), the Canada Foundation for Innovation (CFI) and Ryerson University.

REFERENCES

[1] Lockwood, G. R., Talman, J.R. and Brunke, S. S., "Real-time 3-D ultrasound imaging using sparse synthetic aperture beamforming," IEEE Trans. Ultrason. Ferroelec. Freq. Contr. 45 980–988 (1998)

[2] Turnbull, D. H. and Foster, F. S., "Beam steering with pulsed two dimensional transducer arrays," Ultrasonics, Ferroelectrics and Frequency Control, IEEE Transactions on, vol. 38, no. 4, p. 320±333 (1991)

[3] Jensen, J. A., Nikolov, S. I., Gammelmark, K. L. and Pedersen, M. H., "Synthetic aperture ultrasound imaging," *Ultrasonics*, vol. 44, Supplement, pp. e5-e15, 12/22 (2006).

[4] Chiao, R. Y., Thomas, L. J. and Silverstein, S. D., "Sparse array imaging with spatially-encoded transmits," in *Ultrasonics Symposium, 1997. Proceedings., IEEE*, vol.2, pp. 1679-1682 (1997).

[5] Liu,. R.Y., "Apparatus and method for beamforming in an ultrasonic transducer array," U.S. Patent 4 542 653, Sept. 24 (1985).

[6] Lockwood, G. R., Li, P. C., O'Donnell, M. and Foster, F. S., "Optimizing the radiation pattern of sparse periodic linear arrays," *IEEE Trans. Ultrason., Ferroelect., Freq. Contr.*, vol. 43, pp.7-14 (1996).

[7] Davidsen, R. E., Jensen, J. A., and Smith, S. W., "Two-dimensional random arrays for real-time volumetric imaging, " Ultrason. Imag., vol. 16, pp. 143–163 (1994).

[8] Schwartz, J. L. and Steinberg, B. D., "Ultra sparse, ultra wide band arrays, " IEEE Trans. Ultrason., Ferroelectr., Freq. Contr., vol. 45, no. 2, pp. 376–393 (1998).

[9] Nikolov, S. I. and Jensen. J. A., "Application of different spatial sampling patterns for sparse array transducer design, " Ultrasonics, vol. 37, no. 10, pp. 667–671 (2000).

[10] Yen, J. T., Steinberg, J. P. and Smith, S. W., "Sparse 2-D array design for real time rectilinear volumetric imaging, " IEEE Trans. Ultrason., Ferroelectr., Freq. Contr., vol. 47, no. 1, pp. 93–110 (2000).

[11] Austeng, A. and Holm, S., "Sparse 2-D arrays for 3-D phased array imaging-Design methods, " IEEE Trans. Ultrason., Ferroelect., Freq. Contr., vol. 49, no. 8, pp. 1073–1086 (2002).

[12] Diarra, B., Robini, M., Tortoli, P., Cachard, C., and Liebgott, H., "Design of Optimal 2-D Nongrid Sparse Arrays for Medical Ultrasound" *IEEE Transactions on Biomedical Engineering*, vol. 60, no. 11 (2013).

[13] Karaman, M., Wygant, I. O., Oralkan, Ö. , and Khuri-Yakub, B. T., "Minimally Redundant 2-D Array Designs for 3-D Medical Ultrasound Imaging, " IEEE TRANSACTIONS ON MEDICAL IMAGING, VOL. 28, NO. 7 (2009).

[14] J. A. Johnson , M. Karaman and B. T. Khuri-Yakub , "Coherent array imaging using phased subarrays-Part I: Basic principles" , *IEEE Trans. Ultrason., Ferroelect., Freq. Contr.* , vol. 52 , no. 1 , pp.31 -50 (2005).

[15] Gong, P., A., Kolios, M. C., and Xu, Y., "Delay-encoded transmission and image reconstruction method in synthetic transmit aperture imaging, " *IEEE transactions on ultrasonics, ferroelectrics, and frequency control*, vol. 62, pp. 1745-56 (2015).

[16] Moon, T. K. and Stirling,W. C., "Mathematical Methods and Algorithms for Signal Processing," Upper Saddle, NJ:Prentice Hall (2000).

[17] Jensen, J. A., "Field: A program for simulating ultrasound systems," *Med. Biol. Eng. Co* River *mput.,* vol. 34, pp. 351-353 (1996).

[18] Montaldo, G., Tanter, M., Bercoff, J., Benech, N. and Fink, M., "Cohenrent plane-wave compounding for very high frame rate ultrasonograophy and transient elastography" *IEEE Transactions on ultrasonics, ferroelectrics, and frequency control*, vol.56,p.489 (2009).